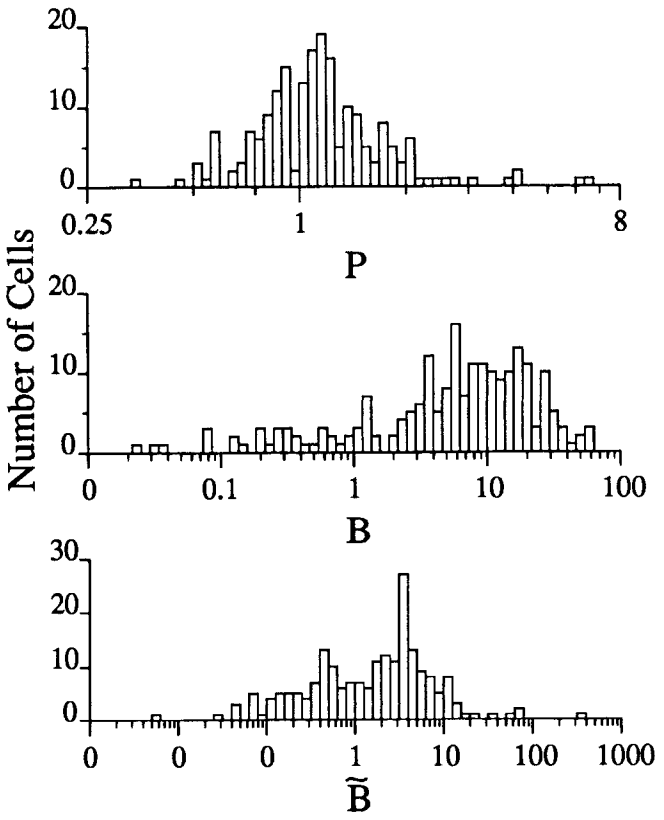

Figure 3. Frequency histograms for our database of 212 MT cells for P, the measure of the shape of $S'(f)$, and two measures of burstiness, B and $\tilde{B}$, averaged over trials for all c. The *top two plots* show that the distribution of cells with respect to the statistics P and B (the fraction of the ISI in the 1, 2, and 3 msec bins) is primarily a continuum. The dip near 1.0 in the distribution of P is an artifact of the classification of cells as burst or nonburst (see Methods). All burst cells have $p > 1.0$; nonburst cells, $p < 1.0$; and mixed cells that are neither one or the other have P near 1.0. The distribution of B has a long left tail due to cells that rarely fire a second spike within 3 msec. The *bottom plot* shows the distribution for a second measure of burstiness, $\tilde{B}$, the ratio of the 2 msec bin to the 5 msec bin in the ISI histogram. B and $\tilde{B}$ are highly correlated for our database, but we use B since it is less sensitive to noise than the ratio measure.

the integral within the window summed over all S'_c. The constraint 20 Hz $< f_p <$ 60 Hz is used to keep the window away from the peak at $f = 0$ (i.e., the DC component) and to avoid scanning higher frequencies where peaks are absent. The average value of S'_c within the window will be called the peak level, P_p. A second sliding window is used in a similar, but minimizing, procedure to find the lowest point, or baseline level, at higher frequencies. The location of the lowest point is quantified by f_b, the center of the window, and the average value within the window, P_b, will be called the baseline level. We constrain f_b to be greater than f_p and less than the cutoff frequency, 500 Hz. All windows are seven spectral bins wide (3.9 Hz/bin) and therefore sacrifice accuracy of localization for noise immunity.

Once the peak frequency f_p and the baseline frequency f_b are determined, a cell is classified as a *burst cell* (below we explain the link between peaks and burst firing) if for at least 90% of all c values $P_p > P_b$, that is, if at nearly all coherence levels, the spectrum has a peak in the 20–60 Hz range. If a cell fails to be classified as a burst cell, then we attempt to localize a dip in the power spectrum [see arrow on $S'(f)$, Fig. 2, cell *d*, bottom right, which has a dip near 20 Hz] using another sliding window. We take f_d to be the center frequency of the seven-bin window that minimizes the integral within the window summed over all c, where 20 Hz $< f_d <$ 500 Hz. We take the average value of the spectra within a window centered at f_d to be P_d. We classify a cell as *nonburst* if for at least 90% of all c values $P_d < 1.0$, that is, if at nearly all coherence levels the spectrum has a dip below the expected baseline level (which manifests itself at high frequencies) for a Poisson-like spike train, which is 1.0 due to our spike rate normalization. This definition would result in classifying a cell with Poisson-distributed spikes (that therefore has a flat power spectrum) as neither burst nor nonburst, but since all cells studied here show evidence of refractory periods, this case does not occur in practice. Note that for a pacemaker cell "oscillating" in the 20–60 Hz band, P can become arbitrarily large as the oscillation becomes increasingly regular.

If a cell fails to be classified as either burst or nonburst, it is classified as *mixed* since at some c values it lacks a significant peak, while at others it lacks a significant dip, in the 20–60 Hz range. To avoid classifying a cell based on too little data, trials with less than six spikes in the 336–2000 msec time window are discarded, and c values with less than eight valid trials are not represented in the set of spectra. Finally, a classification is made only when there are at least three different c values with valid S'_c. Typically, there are six S'_c for $c < 0$, six for $c > 0$, and one for $c = 0$.

A measure of the shape of the power spectrum, P, is associated with each classified neuron. For burst cells, the ratio of the peak to the baseline is used: $P = P_{\text{burst}} = P_p/P_b$. For nonburst cells, the ratio of the dip level to the ideal baseline, 1.0, is used: $P = P_{\text{nonburst}} = P_d$. The value for mixed cells depends on the subcategorization; that is, P follows the definition for burst if S'_c had a peak for the majority of c values but follows the definition for nonburst otherwise. When discussing the shape of power spectrum, we will simply refer to P when the particular definition is understood from context.

Other methods. The PSTHs are computed from the single-trial data by averaging over all trials with identical stimulus conditions, using a bin width of 10 msec. They are normalized to show spike rate rather than counts per bin. Interspike interval (ISI) distributions are computed with 1 msec bin width. Power spectra, $S'(f)$, are usually normalized to match continuous spectra under the assumption that spikes can be described as Dirac δ-functions. In this case, the vertical offset is roughly proportional to the spike rate, and for nonburst cells, the flat level at higher frequencies is usually an accurate reflection of the spike rate, as in Figure 12. Under the second spike-rate normalization (discussed above), spectra are divided by the average spike rate so that all are nearly the same height to allow comparison of shapes, as in Figure 5.

Vertical truncation of histogram plots is indicated by open histogram bars near the top of the graph (Figs. 2, bottom; 5, upper left; 15, both ISI plots and lower right; 18, lower left and right).

Results

Experimental results

We begin by describing the population of MT cells with respect to two statistical measures of the temporal fine structure of spike trains: the ISI distribution and the power spectrum $S'(f)$. The first measure is an order-independent statistic since it contains no information about the temporal order in which the intervals occur. For instance, all short intervals could have occurred at the beginning of each trial and all long intervals at the end, or each short interval could have been followed by a long one. The estimate $S'(f)$ is order dependent since it depends on temporal relationships between events at scales beyond single intervals. Although many different $S'(f)$ may be associated with a particular ISI distribution, we find for this database that the shape of the ISI distribution predicts the shape of the power spectrum quite well, and that the tendency of a cell to fire bursts of action potentials is the basis for the prediction.

Estimates of the ISI and $S'(f)$ are shown in Figure 2 for four cells from the database. Segments of typical spike trains from each cell are shown at the top, and below them, the PSTHs show that the average firing rate is relatively constant throughout the period over which we compute the ISIs and power spectra, from 336 to 2000 msec. Although not shown here, including the initial transients had little effect on the shape of $S'(f)$. The autocorrelation functions, $R'(t)$ (not shown), for these cells do not show ringing, even when the associated spectrum $S'(f)$ has a prom-